Communication

A Coordination Network That Catalyzes O-Based Oxidations

Jong Woo Han, and Craig L. Hill

J. Am. Chem. Soc., **2007**, 129 (49), 15094-15095 • DOI: 10.1021/ja069319v

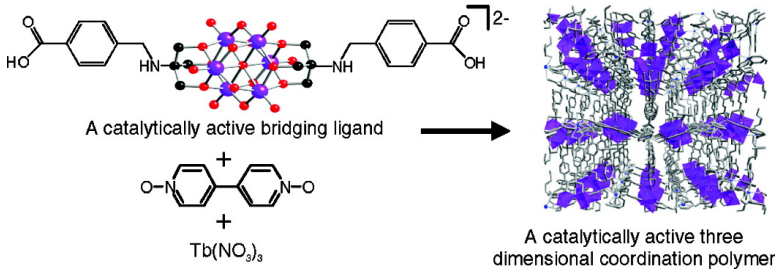

More About This Article

Additional resources and features associated with this article are available within the HTML version:

- Supporting Information
- Access to high resolution figures
- Links to articles and content related to this article
- Copyright permission to reproduce figures and/or text from this article

View the Full Text HTML

J|A|C|S
COMMUNICATIONS

Published on Web 11/17/2007

A Coordination Network That Catalyzes O_2-Based Oxidations

Jong Woo Han and Craig L. Hill*

Department of Chemistry, Emory University, Atlanta, Georgia 30322

Received December 27, 2006; Revised Manuscript Received November 6, 2007; E-mail: chill@emory.edu

Materials that could selectively entrap deleterious compounds (pollutants, toxic agents, etc.) and then catalyze the degradation of these sequestered molecules using only the ambient environment (ideally air at ambient temperature and pressure) would have value in a range of protection, decontamination, and other technologies. A number of impressively porous coordination networks have now been made and the syntheses, architectural possibilities, and some sorption (gas storage, separation, etc.) applications of these materials are promising.[1−5] At the same time, applications of these materials in catalysis has met with limited success to date.[6−11] One reason is that the transition-metal centers in these networks are generally coordinatively saturated. Catalysts, particularly heterogeneous ones, for selective aerobic oxidations are as rare as they are of potential value.[12−14] We report here the preparation and properties of an open-framework coordination network that catalyzes the oxidation of organic reactants by *t*-butyl hydroperoxide (TBHP) and, more significantly, by O_2/air.

The unit, $[V_6O_{13}\{(OCH_2)_3C(NHCH_2C_6H_4\text{-}4\text{-}CO_2)\}_2]^{4-}$ (**1**), made by condensation of tris(hydroxymethyl)amino methane with *p*-chloromethyl benzoic acid, contains a redox active bis(triester)-hexavandate moiety and two carboxylate termini (see Supporting Information, SI). Reaction of **1** with Tb(III) ions and the linking agent 4,4′-bis(pyridine-*N*-oxide) (bpdo) produces the highly crystalline catalytic network with large pores occupied by solvent molecules, $Tb[V_6O_{13}\{(OCH_2)_3C(NH_2CH_2C_6H_4\text{-}4\text{-}CO_2)\}\{(OCH_2)_3C\text{-}(NHCH_2C_6H_4\text{-}4\text{-}CO_2)\}_2]$ (**Tb1**) in 43% yield (see SI). Unit **1** was the logical choice as a catalytic connector because the alkoxy groups of chelating triester-trivanadate units[15] are very stable to hydrolysis and bis(triester)hexavanadate units have extensive reversible redox chemistry.[16,17] Synthesis and crystallization of **Tb1** required very slow diffusion of the reactants together using three liquid layers: a $Tb(NO_3)_3$ solution (DMF/EG = 1:1) at the bottom, a mixed solvent (DMF/EG = 2:1) separation layer in the middle, and bpdo and $TBA_2[H_2\mathbf{1}]$ in DMF at the top (layered over the mixed solvent layer). Use of dense and viscous ethylene glycol further facilitates slow diffusion of the reactants. The crystallization conditions were optimized by varying the density of the layers and the height of the central separating solvent layer. **Tb1** is slightly soluble in DMSO, DMF, and DMA, and insoluble in MeOH, CH_3CN, and non-coordinating solvents such as chloroform and 1,2-dichloroethane.

Two-dimensional (2D) layers comprising Tb(III) centers and bpdo units are linked by **1** into the three-dimensional (3D) coordination network of **Tb1** (Figure 1a). This is a metal−organic framework self-assembly approach somewhat analogous to the "pillared layer" one elaborated by Kitagawa and co-workers.[18,19] In **Tb1** there are two independent interpenetrating 3D networks (Figure 1b). Microporous channels are formed along the crystallographic *a*-axis (Figure S2). In the largest channel, the longest and shortest dimensions are 8.0 and 5.2 Å, respectively. Each Tb(III) center in **Tb1** is approximately dodecahedrally coordinated:

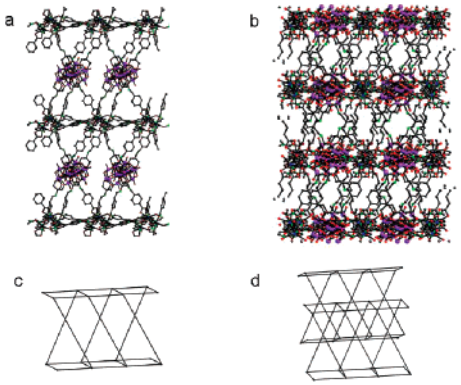

Figure 1. Schematic description of the network connectivity in **Tb1**. (a) The 3D network constructed by linking two-dimensional sheets of Tb(III) centers and bpdo connectors in the third dimension by units of **1**, (b) the overall interpenetrating network structure, (c) a simplified scheme of the 3D connectivity, and (d) a simplified scheme of the overall interpenetrating network structure.

4 bpdo units each contribute one oxygen and 2 bidentate benzoic acid moieties each contribute two oxygens (Figure S1).

In **1**, the bis(triester)hexavanadate moiety is 2- and each carboxylate is 1-. Since there is no nitrate or other anions in the unit cell of **Tb1**, it is reasonable that one of the two secondary amines in **1** is protonated making the **1** unit inside the **Tb1** network bear a charge of 3− which balances the 3+ charge on the Tb center. This assumption is supported by the single-crystal X-ray structure,[20] elemental analysis,[21] and the IR spectrum.[22]

Thermogravimetric analysis (TGA) on the as-synthesized **Tb1** shows a loss in the total weight of 5% from 30 to 90 °C and another 7% from 90 to 180 °C; above 200 °C weight loss with decomposition is continuous (Figure S4). Because of the limited thermal stability of **1** and a large number of the nonvolatile DMF and ethylene glycol solvent molecules in the pores of the as-synthesized **Tb1**, there is no clear distinction between solvent loss and decomposition of the covalent network from the TGA curve. The limited thermal stability of **Tb1** precludes complete removal of the solvent molecules in a vacuum of 10^{-3} Torr. ^{1}H NMR shows that ca. 0.5 DMF molecule per formula unit remains in **Tb1** after such treatment. A weight loss of the partially evacuated **Tb1** from 30 to 120 °C is associated with loss of the residual DMF in the pores. The differential scanning calorimetry (DSC) data support the implications of the TGA data (Figure S5). The IR spectra of **Tb1** collected as a function of temperature are also consistent with the implications of the TGA data (Figure S6).

The solvent-accessible internal volume of **Tb1** is 50.5% of the crystal volume as calculated by PLATON,[23] but DMF molecules in the pores render N_2 adsorption minimal (adsorption isotherms show nonporous behavior at 78 K). However, CO_2 gas adsorption isotherms at different temperatures indicate an activated process involving displacement of DMF solvent molecules in the pores with CO_2 and some porosity at higher temperatures (e.g., 30 m^2/g at

10.1021/ja069319v CCC: $37.00

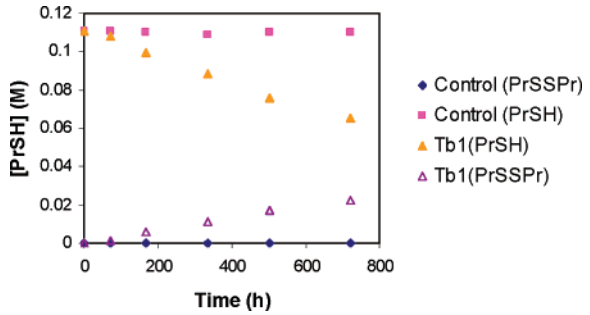

Figure 2. Aerobic oxidation of PrSH catalyzed by **Tb1**. PrSH (0.662 mmol, 0.220 M) decane (internal standard), and the catalyst (0.0074 mmol or milliequivalents of V_6 units in **Tb1**), were stirred in chlorobenzene in a Schlenk tube fitted with a PTFE plug under air at 45 °C. The control reaction shown was run under identical reaction conditions except without the catalyst, **Tb1**. See text for results of other control reactions.

273 K).[24] Although this surface area is still much smaller than the PLATON calculated void volume because of the residual DMF molecules in the pores, the CO_2 adsorption data show that **Tb1** can uptake some guest molecules including potential targets for catalytic oxidative decontamination.

Tb1 catalyzes sulfoxidation by peroxides (rates are increased several-fold over the **Tb1**-free control reactions; see SI) but more importantly, **Tb1** catalyzes O_2-based oxidations and does so under very mild conditions. The aerobic oxidation of PrSH, a model for odorants and mild toxics ubiquitous in human environments, was examined (Figure 2). **Tb1** catalyzes eq 1 producing 18.5 turnovers based on the molar equivalents of V_6 groups in the **Tb1** (41% yield of the desired nonodorous disulfide at 45 °C after 30 days), *using*

$$2\mathrm{PrSH} + 0.5\mathrm{O_2} \rightarrow \mathrm{PrSSPr} + \mathrm{H_2O} \qquad (1)$$

only ambient air as the oxidant. Four control reactions were run: (1) no catalyst, (2) $TbCl_3$ only, (3) a strong acid (*p*-TsOH) only (all three gave no disulfide) and (4) an equivalent molar quantity of soluble monomer, **1** (half as active as insoluble **Tb1**). **Tb1** can be isolated and reused without loss of catalytic activity while the supernatant shows no catalytic activity. The IR spectra (Figure S11) and X-ray powder diffraction patterns (Figure S3) of **Tb1** collected before and after the catalytic reactions indicate the framework structure is maintained under turnover conditions. Kinetic studies of eq 1 catalyzed by **Tb1** indicate that the rate is first order in both PrSH and **Tb1** (Figures S9 and S10) but independent of the partial pressure of O_2. The same reaction (PrSH + **Tb1**) under N_2 results in reduction of the hexavanadate units (indicated by the change in color from orange to green; see SI) and subsequent loss of the catalytic activity. Adding O_2 or air reoxidizes the V_6 units. All these findings are consistent with a mechanism involving rate-limiting bimolecular reaction between of PrSH and the V_6 units in **Tb1** primarily on the outside of the particles and fast reoxidation of the reduced V_6 units in **Tb1** by O_2/air.

In summary, we have prepared a rare example of a heterogeneous aerobic oxidation catalyst, **Tb1**, a three-dimensional coordination polymer from a predesigned bis(triester)hexavanadate derivative (**1**), bis(pyridine-*N*-oxide) (bpdo), and Tb(III) ions. Catalytic turnover does not disrupt the open-framework structure. However, the channels in **Tb1** are largely blocked by solvent molecules. Thus future work will seek similar open-framework redox-active materials sufficiently robust that the pore solvent molecules can be removed (and commensurately higher porosity and catalytic rates can be seen).

Acknowledgment. We thank the ARO (Grant W911NF-05-1-0200) and TDA Research Corp. (Grant W911NF-04-C-0136) for support and K. I. Hardcastle and X. Fang for X-ray crystallography.

Supporting Information Available: Experimental details, CIF files for squeezed and nonsqueezed **Tb1**, table of crystallographic information of H_2**1** and **Tb1**, space-filling model of channel structure, catalytic data for PrSH and THT oxidation, TGA and DSC for **Tb1**, powder X-ray patterns, and IR data. This material is available free of charge via the Internet at http://pubs.acs.org.

References

(1) Kitagawa, S.; Noro, S.-i.; Nakamura, T. *Chem. Commun.* **2006**, 701−707.
(2) Kitagawa, S.; Kitaura, R.; Noro, S.-i. *Angew. Chem., Int. Ed.* **2004**, *43*, 2334−2375.
(3) Yaghi, O. M.; O'Keeffe, M.; Ockwig, N. W.; Chae, H. K.; Eddaoudi, M.; Kim, J. *Nature* **2003**, *423*, 705−714.
(4) Bradshaw, D.; Claridge, J. B.; Cussen, E. J.; Prior, T. J.; Rosseinsky, M. J. *Acc. Chem. Res.* **2005**, *38*, 273−282.
(5) Moulton, B.; Zaworotko, M. J. *Chem. Rev.* **2001**, *101*, 1629−1658.
(6) Uemura, T.; Kitaura, R.; Ohta, Y.; Nagaoka, M.; Kitagawa, S. *Angew. Chem., Int. Ed.* **2006**, *45*, 4112−4116.
(7) Dybtsev, D. N.; Nuzhdin, A. L.; Chun, H.; Bryliakov, K. P.; Talsi, E. P.; Fedin, V. P.; Kim, K. *Angew. Chem., Int. Ed.* **2006**, *45*, 916−920.
(8) Cho, S.-H.; Ma, B.; Nguyen, S. T.; Hupp, J. T.; Albrecht-Schmitt, T. E. *Chem. Commun.* **2006**, 2563−2565.
(9) Wu, C.-D.; Lin, W. *Inorg. Chem.* **2005**, *44*, 1178−1180.
(10) Seo, J. S.; Whang, D.; Lee, H.; Jun, S. I.; Oh, J.; Jeon, Y. J.; Kim, K. *Nature* **2000**, *404*, 982−986.
(11) Fujita, M.; Kwon, Y. J.; Washizu, S.; Ogura, K. *J. Am. Chem. Soc.* **1994**, *116*, 1151−1152.
(12) (a) Neumann, R.; Levin, M. *J. Am. Chem. Soc.* **1992**, *114*, 7278−7286 and references therein. (b) Brink, G.-J.; Arends, I. W. C. E.; Sheldon, R. A. *Science* **2000**, *287*, 1636−1639 and references therein. (c) Nishiyama, Y.; Nakagawa, Y.; Mizuno, N. *Angew. Chem., Int. Ed.* **2001**, *40*, 3639−3641 and references therein. (d) Botar, B.; Geletii, Y. V.; Kögerler, P.; Musaev, D. G.; Morokuma, K.; Weinstock, I. A.; Hill, C. L. *J. Am. Chem. Soc.* **2006**, *128*, 11268−11277 and references therein..
(13) (a) Rhule, J. T.; Neiwert, W. A.; Hardcastle, K. I.; Do, B. T.; Hill, C. L. *J. Am. Chem. Soc.* **2001**, *123*, 12101−12102. (b) Okun, N. M.; Anderson, T. M.; Hardcastle, K. I.; Hill, C. L. *Inorg. Chem.* **2003**, *42*, 6610−6612. (c) Okun, N. M.; Anderson, T. M.; Hill, C. L. *J. Am. Chem. Soc.* **2003**, *125*, 3194−3195.
(14) Vasylyev, M.; Neumann, R. *Chem. Mater.* **2006**, *18*, 2781−2783 and work cited therein.
(15) Hou, Y.; Hill, C. L. *J. Am. Chem. Soc.* **1993**, *115*, 11823−30.
(16) Chen, Q.; Goshorn, D. P.; Scholes, C. P.; Tan, X. L.; Zubieta, J. *J. Am. Chem. Soc.* **1992**, *114*, 4667−4681.
(17) Han, J. W.; Hardcastle, K. I.; Hill, C. L. *Eur. J. Inorg. Chem.* **2006**, 2598−2603.
(18) Maji, T. K.; Uemura, K.; Chang, H.-C.; Matsuda, R.; Kitagawa, S. *Angew. Chem., Int. Ed.* **2004**, *43*, 3269−3272.
(19) Kitaura, R.; Fujimoto, K.; Noro, S.-i.; Kondo, M.; Kitagawa, S. *Angew. Chem., Int. Ed.* **2002**, *41*, 133−135.
(20) As is the usual case for highly porous materials, the pores of Tb**1** contain many disordered and dynamic solvent molecules which significantly impact the *R* value. To improve the refinement, the SQUEEZE routine of PLATON was applied to treat the diffuse electron density. Crystal data for **Tb1**: monoclinic *P*21/*c*, a = 13.102(4) Å, b = 26.279(9) Å, c = 26.104(6) Å, β = 93.923(5)°, V = 8967(5) Å, Z = 4, Mo Kα (0.71073 Å) radiation (T = 100 K), R1 = 0.1378 [0.0879], wR2 = 0.3474 [0.2295] with $I > 2\sigma(I)$. Statistics after using SQUEEZE are bracketed.
(21) Elemental analysis for **Tb1**: [Tb(bpdo)$_2$(H**1**)]·1.5DMF·3.0EG. Anal. Calcd for $C_{54.5}H_{71.5}N_{7.5}O_{34.5}V_6Tb$: C, 35.42; H, 3.90; N, 5.68; V, 16.5; Tb, 8.6. Found: C, 35.51; H, 4.02; N, 5.60; V, 16.0; Tb, 8.5.
(22) IR shows no typical vibrational band from NO_3^- (D_{3h}) 1734−1790, 1300−1550, 801−834 cm^{-1}; KNO_3 has 1770, 1360, and 827 cm^{-1}). Nyquist, R. A.; Putzig, C. L.; Leugers, M. A. *The Handbook of Infrared and Raman Spectra of Inorganic Compounds and Organic Salts*; Academic Press: San Diego, CA, 1997; Vol. 4.
(23) Spek, A. L. *J. Appl. Crystallogr.* **2003**, *36*, 7−13.
(24) Adsorption is an exothermic process so as the temperature is raised the amount of sorption generally decreases. However, constrictions in very small micropores constitute an energy barrier to the adsorbate's passage through the pores, resulting in an activated uptake. Gregg, S. J.; Sing, K. S. W. *Adsorption, Surface Area and Porosity*, 2nd ed.; Academic Press: London, 1982.

JA069319V